SHOCK, Vol. 51, No. 5, pp. 557–568, 2019

SURFACTANT PROTEIN D DAMPENS LUNG INJURY BY SUPPRESSING NLRP3 INFLAMMASOME ACTIVATION AND NF-κB SIGNALING IN ACUTE PANCREATITIS

Jia Yu,[*†] Lan Ni,[†] Xiaoyi Zhang,[†] Jing Zhang,[†] Osama Abdel-Razek,[†] and Guirong Wang[†]

[*]Department of Hepatobiliary Surgery, Renmin Hospital of Wuhan University, Wuhan, Hubei Province, People's Republic of China; and [†]Department of Surgery, SUNY Upstate Medical University, Syracuse, New York

Received 24 May 2018; first review completed 8 Jun 2018; accepted in final form 27 Jul 2018

ABSTRACT—Severe acute pancreatitis (SAP) often causes acute lung injury (ALI) by systemic inflammatory response. Surfactant protein D (SP-D) plays critical roles in host defense and inflammation regulation. NLRP3 inflammasomes and NF-κB signaling are key regulators in innate immunity and inflammation. We hypothesized that SP-D attenuates ALI by suppressing NLRP3 inflammasome and NF-κB activation. **Methods:** Wild-type C57BL/6 (WT), SP-D knockout (KO), and humanized transgenic SP-D (hTG) mice were used in this study. SAP was induced by administration of one-dose lipopolysaccharide (10 mg/kg) and 6 hourly intraperitoneal injections of cerulein (Cn) (100 μg/kg). Animals were killed 6 and 24 h after first Cn treatment. Histopathologic changes in pancreas and lung were assessed by light and electron microscopes. Serum amylase, IL-1β, IL-6, and MCP-1 levels were determined by kit/ELISA. NLRP3 inflammasome, NF-κB, and MPO activations were analyzed by western blotting and immunofluorescence. **Results:** KO mice showed more severe pancreatic and lung injury than WT mice in SAP. hTG mice exhibited similar degree in lung injury as WT mice. Mitochondrial and rough endoplasmic reticulum damages, autophagosome formation were observed in the alveolar type II and acinar cells of SAP mice. SAP KO mice had increased bronchoalveolar lavage fluid inflammatory cells, higher levels of serum IL-1β, IL-6, and MCP-1 than SAP WT and hTG mice. Levels of NLRP3 inflammasome (NLRP3, ASC, and Caspase-1) and NF-κB activation in SAP KO mice were higher than SAP WT and hTG mice. **Conclusion:** SP-D exerts protective effects against ALI via suppressing NLRP3 inflammasome and NF-κB activation in experimental SAP.

KEYWORDS—Acute lung injury (ALI), acute pancreatitis (AP), NF-κB signaling, NLRP3 inflammasome, surfactant protein D (SP-D)

INTRODUCTION

Acute pancreatitis (AP) is a complex inflammatory reaction of the pancreas, followed by the multiple organ damage (1). Acute lung injury (ALI) that clinically manifests as acute respiratory distress syndrome (ARDS) is common in critically ill patients due to various conditions including severe acute pancreatitis (SAP), and it seems to be the predominant cause of death (2). These conditions have been characterized by the macrophage and neutrophil accumulation in the lung and the production of inflammatory mediators, including complement activation products, cytokines and chemokines, and oxidants. Vascular endothelial and alveolar epithelial cell damage/death leads to disruption of the blood-alveolar barrier, resulting in pulmonary edema, intrapulmonary hemorrhage, and severely impaired gas exchange (3). Accumulated evidence demonstrates that its basic etiology is tissue destruction accompanied by unresolved inflammation and disordered cellular pathways (4). Specific and effective interventions for this disease are not available largely because of a lack of understanding of the early cellular events and molecular mechanisms in its inflammatory pathophysiology.

Recent studies demonstrated that the inflammatory cascade initiated by sterile inflammation and mediated by inflammasome activation is a central component in a wide range of diseases, including AP and ALI (5–7). Among the various inflammasome complexes identified thus far, the Nod-like receptor pyrin domain-containing protein 3 (NLRP3) inflammasome is considered to be an integrator of diverse sterile and some nonsterile injury signals, as well as the primary regulator of the resultant immune response (7). The NLRP3 inflammasome refers to a family of macromolecular protein complexes composed by NLRP3, and apoptosis-associated speck-like protein containing a caspase recruitment domain (ASC) and caspase-1.

The interdependent relationship between oxidative stress and tissue injury in Cn-induced AP is supported by numerous studies (8). The pathogenesis of ALI/ARDS, a major clinical syndrome with limited therapy and high mortality, has already been proven to be closely related to oxidative stress and inflammation (9). It is not only inflammation induced by oxidative stress but also oxidative stress that accelerates inflammation through the activation of proinflammatory pathways, such as the NLRP3 inflammasome and nuclear factor-kappa B (NF-κB) signaling (10). NLRP3 inflammasome, one of the most well-characterized inflamasomes, is an oligomeric molecular complex that can be activated by diverse ''danger signals''

Address reprint requests to Guirong Wang, PhD, Department of Surgery, UH Room 8715, SUNY Upstate Medical University, 750 E Adams St, Syracuse, NY 13210. E-mail: wangg@upstate.edu

This work was supported by NIH R01HL136706 and NSF research award (1722630) (to GW), as well as the National Natural Science Foundation of China (Grant no. 81300356) (to JY).

This study was selected as one of the New Investigator Nominees at the 41st Annual Conference on Shock, held in Scottsdale, Arizona, June 9–12, 2018.

The authors report no conflicts of interest.

DOI: 10.1097/SHK.0000000000001244

(e.g., ATP and ROS) (11). NF-κB, a ubiquitous inducible transcription factor, is a robust regulator of various proinflammatory cytokine gene expressions in response to external stimuli. They include several important proinflammatory cytokines such as IL-1β, IL-6, TNF-α, and chemokines such as monocyte chemoattractant protein-1 (MCP-1/CCl2) (12, 13). Intriguingly, the NF-κB signaling pathway does not merely act as a classical proinflammatory pathway with a conventional mode of action but also provides a novel insight due to its critical role in the initial step of NLRP3 activation (14).

The inflammatory response in the alveolar microenvironment is tightly regulated to avoid damage to the gas-exchanging delicate structures through the concerted efforts of the innate and adaptive immune system (15). Two important components of the innate immune response are alveolar macrophages (AMs) and pulmonary surfactants in the lung, the latter of which regulates macrophage function (15). Innate immune molecule surfactant protein D (SP-D), a member of C-type lectin family, plays indispensable roles in host defense, regulation of inflammation and homeostasis in the lung. Immune-related functions regulated by SP-D include agglutination of pathogens, phagocytosis, oxidative burst, antigen presentation, cytokine secretion, modulation of apoptosis, and clearance of apoptotic cells (16). Although initially predominant expression of SP-D was identified in alveolar type II (AT II) epithelial cells of lung, extrapulmonary existence of SP-D has been reported (17). SP-D can opsonize pathogens and foreign particles that may be deposited in the lungs and then interacts with the alveolar macrophages via a series of cellular receptors, leading to their uptake and downstream immune response (18). Humanized transgenic (hTG) mice with lung-specific SP-D expression provide a powerful tool to study organ-specific SP-D role in SAP.

Previous studies demonstrated the protective roles of SP-D and the harmful effects of overexpressing NLRP3 and NF-κB signaling in the context of ALI/ARDS (19–21). Among the cellular response mechanisms, SP-D is considered a survival factor that alleviates oxidative injury, whereas both the NLRP3 and NF-κB pathways are proinflammatory pathways that cause cellular damage. These pathways are implicated in the development and resolution of ALI (10). Our recent studies demonstrated that SP-D is involved in the regulation of NF-κB signaling pathway in sepsis-induced acute pancreatic and kidney injury (22, 23). However, there is no evidence to elucidate how SP-D interacts with the NLRP3/NF-κB pathways and how SP-D protects against ALI associated with AP. Therefore, we hypothesized that SP-D can attenuate lung inflammation and injury by suppressing NLRP3 inflammasome activation and regulating NF-κB signaling pathway in an experimental SAP model induced by Cn plus lipopolysaccharide (LPS) treatment.

MATERIALS AND METHODS

Animals

Wild-type mice (8–12 weeks old, C57BL/6) were obtained from Jackson Laboratories (Bar Harbor, ME) and acclimated for at least a week before starting the experiments. SP-D knockout (SP-D KO) mice with C57BL/6 background were kindly provided by Dr. Hawgood's laboratory of the University of California, San Francisco. Humanized transgenic SP-D (hTG, with lung-specific human SP-D expression without mouse SP-D background) mice were generated by our laboratory and were used in this study. The SP-D KO mice were backcrossed at least 10 generations against a C57BL/6 background. The genotypes of all mice used in this study were determined by PCR analysis with mousetail DNA. No significant difference of phenotype exists between age- and sex-matched WT, SP-D KO, and hTG SP-D mice. All the animals were housed at the central animal facilities, and were maintained on a normal 12 h/12 h light/dark cycle at 24°C with regular mouse chow (Catalog#0006539, LabDiet, St. Louis, Mo) and water *ad libitum*. Mice were fasted overnight before induction of pancreatitis. All experiments and animal handling were approved by Institutional Animal Care and Use Committee at SUNY Upstate Medical University (IACUC #410), and meet the National Institutes of Health and ARRIVE guidelines on the use of laboratory animals. Both male and female mice were used in this study.

SAP model

All mice were fasted for 12 h, and the model of SAP induced by Cn and LPS in this study was previously described with a minor modification. Our previous study indicated that the mice exhibited mild pancreatitis after treatment with Cn alone at a dosage (100 μg/kg/h for 6 hourly intraperitoneal injections) (24). A severe form of acute pancreatitis, characterized by local organ injury and distinct organ damages or dysfunctions, can be induced by a relatively minor secondary insult (administration of a small dose of LPS) (5). Therefore, in this SAP model, the mice (WT, SP-D KO, and hTG SP-D) were treated with Cn (Sigma, St Louis, Mo) plus LPS group (Cn + LPS, SAP group). In brief, mice were given 6 hourly intraperitoneal injections of Cn at 100 μg/kg and one intraperitoneal injection of LPS (10 mg/kg; from *Escherichia coli* 026:B6; Sigma) immediately after the first injection of Cn. Animals in the control (Cntl) group received same size of normal saline. Mice were killed 6 and 24 h after the first Cn injection.

Mouse specimen collection

To collect the mouse blood and other tissues, mice were first anesthetized using intraperitoneal ketamine/xylazine (90 mg/kg ketamine, 10 mg/kg xylazine) injection and then euthanized. Blood was collected from the inferior vena cava using 1-mL syringe. The pancreas and lung were fixed for histological analysis or frozen in liquid nitrogen immediately for western blotting analysis. In addition, the lungs of some mice were lavaged for bronchoalveolar lavage fluid (BALF) and cell analysis (see later).

Alpha-amylase activity assay

Alpha-amylase activity of serum was determined using an amylase colorimetric assay kit (Sigma).

Serum cytokine and chemokine determination

The levels of IL-1β, IL-6, and MCP-1 (CCl2) in serum were determined using commercially available murine enzyme-linked immunosorbent assay (ELISA) kits following the manufacturer's instructions (ThermoFisher Scientific Inc., Pittsburgh, Pa). All samples were analyzed in triplicates.

Cell counting in BALF

BALF was prepared for quantification of inflammatory cells in a separate group of experimental animals. To perform BAL, 0.5 mL saline was instilled via trachea and then gently withdrawn; it was repeated for 3 times. Normally, a total of 1.2 mL of BALF was obtained from each mouse lung. Total cell counts in BALF were determined with a hemocytometer. The BALF samples were centrifuged at 250 × *g* for 10 min and then cells were resuspended in 1 mL of sterile saline (4°C). One hundred microliter of diluted cell solution was mounted on a slide by cytospin centrifugation at 1,000 rpm for 3 min. Slides were stained using the Protocol HEMA-3 cell staining kit (ThermoFisher Scientific Inc.). Macrophages/monocytes and polymorphonuclear neutrophils (PMNs) in the BALF were identified and quantified by Nikon 2000 research light microscope (×200 magnification).

Histopathological analysis

Murine pancreas and lung were fixed in 10% formalin for at least 24 h and embedded in paraffin. About 4-μm (pancreas) and 5-μm (lung) sections were processed for hematoxylin–eosin (H/E) staining by standard procedures. Then multiple randomly chosen microscopic fields from at least five mice in each

group were examined by two investigators in a blinded manner. For pancreatic injury, the scoring was on a scale of 0 to 3 (0 being normal and 3 being severe) according to four items: presence of vacuolization, interstitial edema, interstitial inflammation, and number of acinar cell necrosis, as previously described (25). For lung injury, the scoring was performed according to recommendation by the American Thoracic Society (26).

Analysis by transmission electron microscopy

The pancreatic and lung tissues were fixed by 2.5% glutaraldehyde and 2% paraformaldehyde in 0.1 M phosphate buffer (pH 7.4) and further fixed in 1% osmium tetroxide in 0.1 M phosphate buffer (pH 7.4) for 1 h. Samples dehydrated in a graded ethanol series, and embedded in LX-112 (Ladd Research Industries, Vermont, Va). Thin sections (70 nm) were cut by Diatome knife and stained with uranyl acetate and lead citrate. Samples were viewed in a JEOL JEM1400 transmission electron microscopy (TEM) (JEOL USA Inc., Peabody, Mass). Each sample was examined at various magnifications from ×6,000 to 35,000.

Immunofluorescence analysis

Paraffin-embedded sections were incubated at 60°C for 1 h, deparaffinized with xylene twice, and then subjected to graded series of ethanol. Antigen retrieval was performed with sodium citrate buffer (pH 6.0) at boiling point for 10 min. Permeabilization was performed with 0.2% Triton X-100. Sections were subsequently blocked with 10% donkey serum (ab7475; Abcam, Cambridge, Mass) for 50 min at room temperature. Sections were incubated overnight with primary antibodies listed below and then were incubated with Alexa Fluor 488-conjugated Donkey Anti-Rabbit secondary antibody (ab150073; Abcam) at room temperature for 1 h. Nuclei were counterstained with 4,6-diamidino-2-phenylindole (DAPI, ab104139; Abcam).

Antibodies used in immunofluorescence analysis included Anti-SP-D antibody (Dr. Jo Rae Wright of the Duke University Medical Center for mouse SP-D Ab), Anti-$NLRP_3$ antibody (PA5-20838; Thermo Scientific), antibody p-IκB-α (#2859; Cell Signaling Technology [CST], Boston, Mass), p-NF-κB p65 (#3033; CST), Anti-Myeloperoxidase (MPO) antibody (ab9535; Abcam), and IL-1β (ab205924; Abcam). Slides were visualized by a Nikon Research 2000 microscope, analyzed by the Image J software (NIH) for quantitative analysis in at least five randomly selected high-power (×200) fields/slides.

Western blotting analysis

Lung tissues were homogenized in protein lysis buffer containing protease and phosphatase inhibitors. Protein concentrations were determined using the micro-BCA protein assay kit (Thermo Scientific, Rockford, Ill). Protein samples (50 μg) were subjected to separation by reducing SDS-polyacrylamide gel electrophoresis, and then transferred onto PVDF membrane at 4°C overnight (Bio-Rad, Hercules, Calif). The membrane was blocked in 5% nonfat milk in Tris-buffered saline, and probed using a primary antibody against $NLRP_3$ (MA5-20838; Thermo Scientific), or cleaved caspase-1 (#67314; CST), or apoptosis-associated speck-like protein containing CARD (ASC) (#67824; CST), or p-NF-κB p65 (#3033; CST), and subsequently incubated with a secondary HRP-conjugated antibody (Bio-Rad, Hercules, Calif). Bands were detected using Pierce ECL Western Blotting detection reagent (Thermo Scientific) and the blots were exposed to X-film. The membrane was stripped and reprobed with β-actin antibody (ab16039; Abcam) or proliferating cell nuclear antigen (PCNA) (#13110; CST) as an internal control. Antibody-reactive bands were revealed by enhanced chemiluminescence and exposed to radiographic film. The expression of protein was quantified after scanning of films by the Quantity One software (Bio-Rad).

STATISTICAL ANALYSIS

In this study, all the data are expressed as mean ± SEM. Statistical analyses of the data were performed by using one-way analysis of variance (ANOVA) followed by the Student–Newman–Keul test (SPSS, 20.0). $P < 0.05$ was considered to be statistically significant.

RESULTS

SP-D expression in the lung of hTG SP-D mice

hTG SP-D mice were generated and characterized by PCR genotyping and protein expression analyses. The genotyping analysis showed the positive fragment of human SP-D gene but no mouse SP-D gene in the hTG mice (Fig. 1A). Because the transgene hSP-D was driven by 3.7 kb SP-C promoter sequence, the expression of transgene hSP-D is only in alveolar type II cells of the lung (27). We further examined the level of hTG SP-D expression and distribution in the lung using western blot and immunofluorescence analysis. SP-D protein in hTG mice was expressed in the lung and the level of SP-D on western blot was comparable to that of WT mice. As expected, no SP-D protein was detected in SP-D KO mice (Fig. 1, B–D). The results from immunofluorescence analysis indicated that alveolar type II epithelial cells showed positive staining for SP-D expression in both WT and hTG mice but not in the SP-D KO mice (Fig. 1D).

Cn plus LPS-induced SAP model

In the present study we have adapted one SAP model with multiple Cn plus LPS treatments (5). Histopathological analysis showed the injury of pancreas and lung at 6 and 24 h posttreatment but not in control (Fig. 2A). Injured pancreas displayed lobular mesenchymal rarefaction, inflammatory cell infiltration, hemorrhage, and necrosis. Similarly, injured lung showed increased neutrophils in the alveolar space and the interstitial space, proteinaceous debris in the airspaces, and alveolar thickening, and lung histological damage. The injury scores in the pancreas and lung were higher at 24 h than at 6 h after treatment (Fig. 2, B and C), suggesting that hyperamylasemia developed (data shown in Fig. 3E) immediately in this SAP model. Based on the results of time-course experiments, we studied various histopathological, cellular, and molecular parameters of SAP-induced injury among three types of mice at 24 h after treatment in the following experiments.

SP-D reduced the severity of SAP-induced pancreas and lung injury

We analyzed histopathological changes in pancreatic and lung tissues from WT, SP-D KO (KO), and hTG mice at 24 h in SAP model. The results showed that KO mice exhibited more vulnerable to inflammatory injury in the pancreas and lung after SAP. As shown in Figure 3, the severity of pancreatic (Fig. 3A) and lung (Fig. 3B) injury increased in KO mice compared with WT mice. Of interest, hTG mice showed reduced pancreatic and lung injury compared with KO mice in SAP model. The scores of pancreatic and lung injury were higher in KO mice than WT mice and hTG mice, for pancreas, Fig. 3C; KO versus WT and hTG ($P < 0.05$) and for lung, Fig. 3D; KO versus WT and hTG ($P < 0.05$). Furthermore, analysis of serum amylase activity, a common biomarker of pancreatic injury, indicated progressive increase from 6 to 24 h after treatment. KO mice showed higher level of serum amylase activity than WT and hTG mice (Fig. 3E, $P < 0.05$, KO vs. WT and hTG). No differences of serum amylase activity and injury scores of pancreas and lung were observed between SAP hTG and WT mice (Fig. 3, C and D).

Ultrastructural analysis by electron microscopy

Electron microscopy analysis revealed the ultrastructural abnormalities of mitochondria and other organelles in both

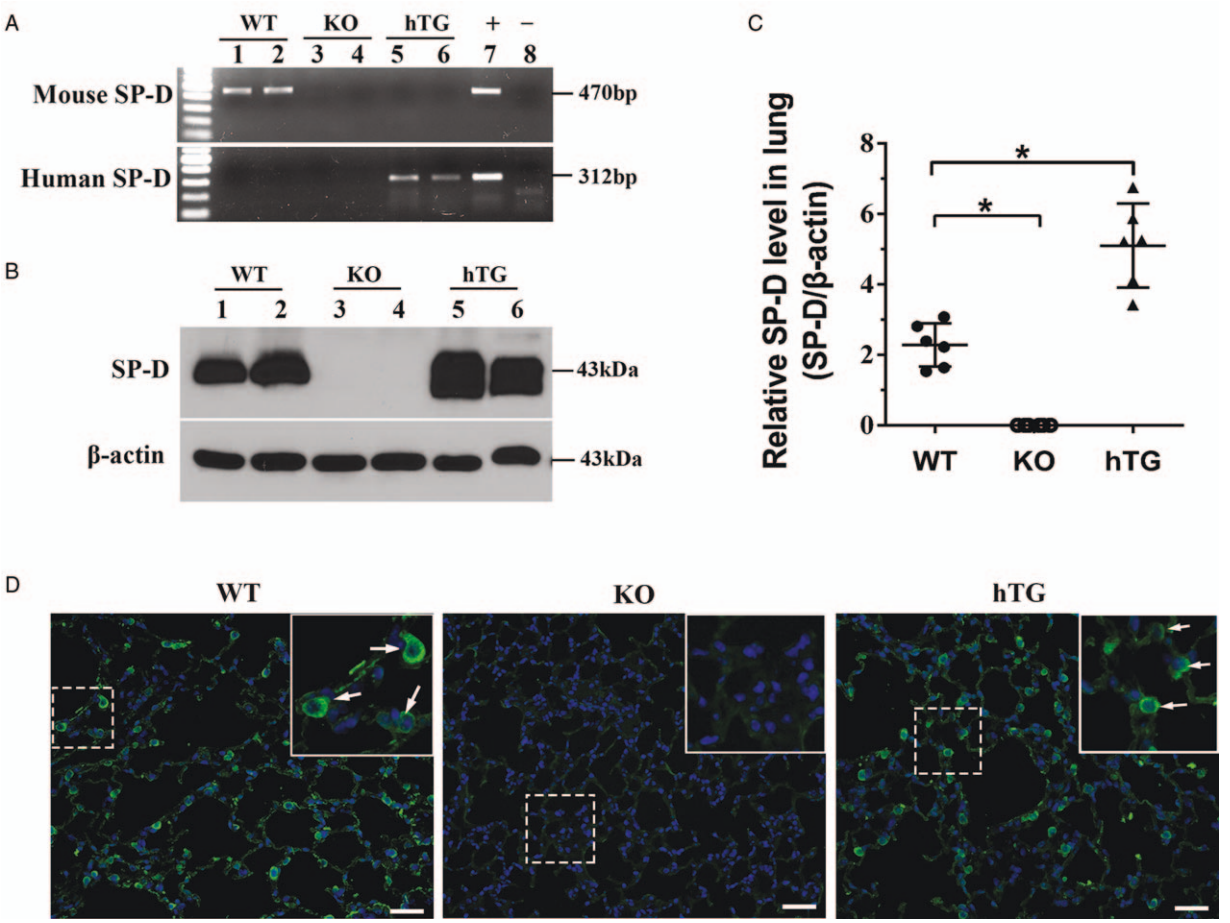

Fig. 1. **Genotyping analysis of hTG SP-D mice and SP-D expression in the lung.** The mouse SP-D (mSP-D) and human SP-D (hSP-D) were analyzed by genotyping with specific PCR amplification in WT, KO, and hTG transgenic mice (A). The sizes of PCR products of mSP-D and hSP-D are 470 bp and 312 bp, respectively. Panel A depicts the results of genotyping analysis: the mice carrying only mSP-D gene are WT mice (lane 1, 2); the mice without mSP-D and hSP-D are SP-D KO mice (lane 3, 4); the mice with hSP-D gene but no mSP-D gene are hTG mice (lane 5, 6). The recombinant plasmid was used as positive control and the KO mouse genomic DNA as negative control. SP-D expression in the lung was examined by Western blotting analysis (B), and quantitative analysis (C), as well as immunofluorescence assay (D). As expected, SP-D was expressed in the lung of WT and hTG mice, but not in KO mice. WT, wild-type mice; hTG, humanized SP-D transgenic mice. Graphs are expressed as means ± SEM; n = 3. $^{*}P < 0.05$. (Original magnification ×200, scale bars = 200 μm).

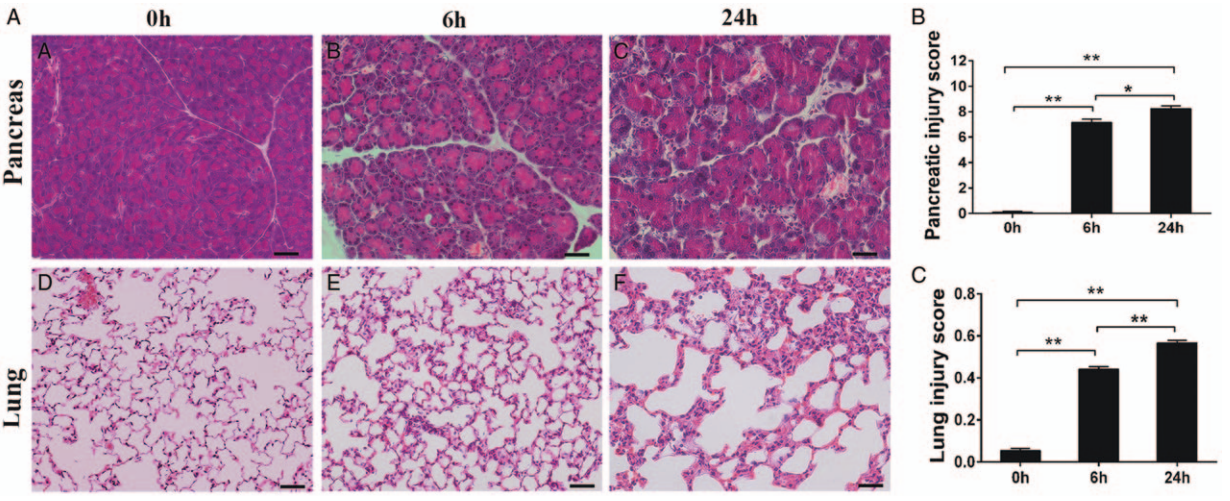

Fig. 2. **Time-course changes of pancreatic and lung injury after cerulein plus LPS treatment.** Representative micrographs of pancreas and lung at 0, 6, and 24 h after cerulein plus LPS treatment are presented; obvious tissue injury in the pancreas and lung are observed (A). Pancreatic (B) and acute lung (C) injury scores were calculated, indicating higher scores of pancreas and lung injury at 24 h than at 6 h after treatment, respectively. Note: "0 h" represents the baseline of these parameters for control group treated with saline. Graphs are expressed as means ± SEM; n = 5. $^{*}P < 0.05$; $^{**}P < 0.01$. (Original magnification ×200, scale bars = 200 μm).

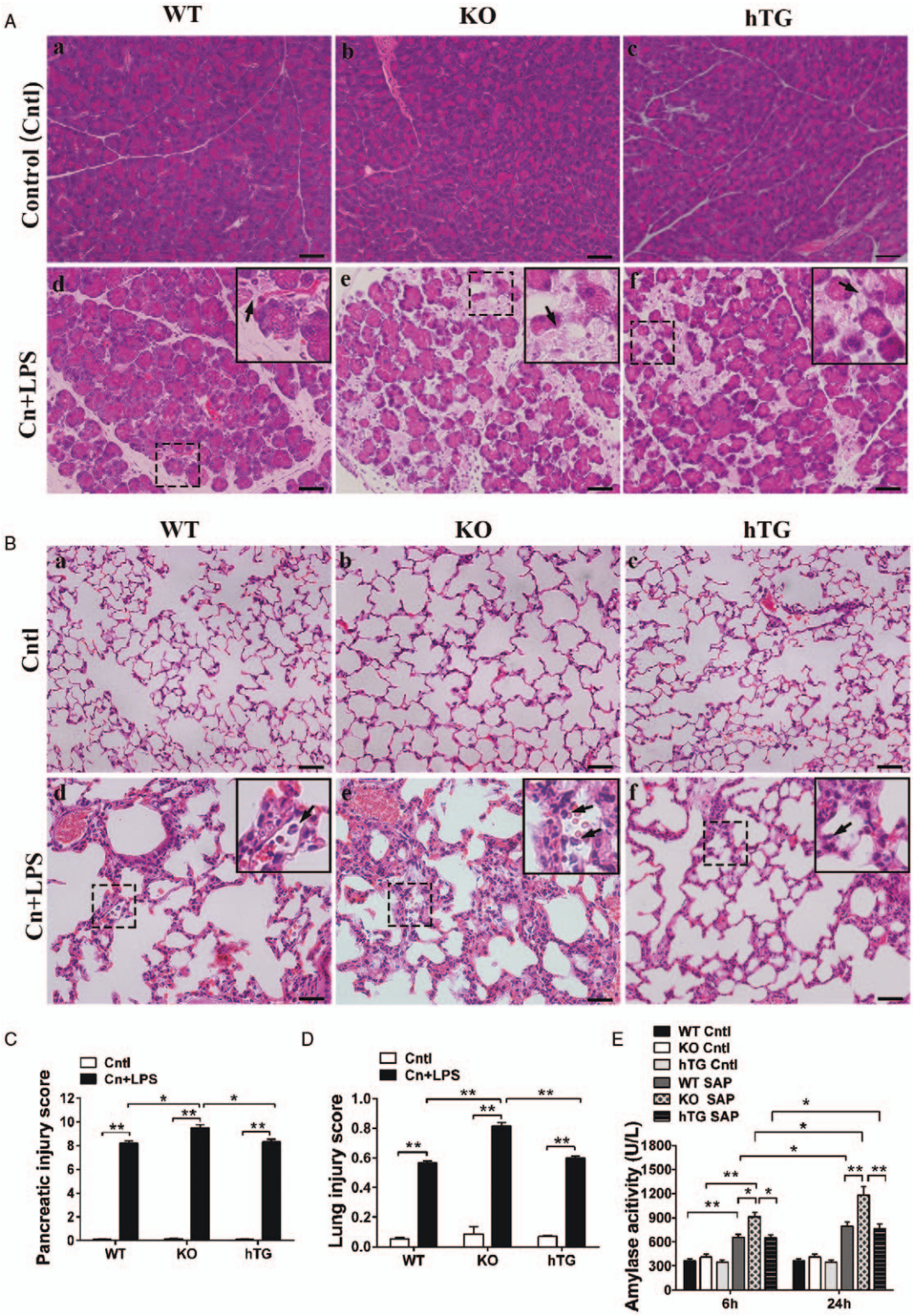

FIG. 3. **Comparison of pancreatic and lung injury and serum amylase activity in SAP WT, KO, and hTG mice.** Representative histological micrographs of pancreas (A) and lung (B) from control (Cntl) and severe acute pancreatitis (SAP; i.e., Cn + LPS) WT, KO, an hTG mice are presented. Acinar cell injury or necrosis (arrows in A) in pancreatic tissue and alveolar congestion, interstitial and alveolar inflammatory cell infiltration (arrows in B) were observed. The scores of pancreatic (C) and lung (D) injury were assessed quantitatively as described in the "Materials and Methods," respectively, and then they are compared in WT, KO, and hTG mice. Panel E depicts the different levels of serum amylase activity at 6 and 24 h after cerulein and LPS treatment in WT, KO, and hTG mice. Graphs are expressed as means ± SEM; n = 6. $^{*}P < 0.05$; $^{**}P < 0.01$. Cntl, Control group; Cn + LPS, cerulein + lipopolysaccharide. (Original magnification ×200, scale bars = 200 μm).

pancreas (Fig. 4, B and D) and lung cells (Fig. 4F) of SAP WT mice but not in the control WT mice (Fig. 4, A, C, and E). These abnormalities consist not only of a decreased number of mitochondria but also of an enlarged and abnormal shape, variations in the number of cristae and particular patterns of cristae, and abnormal inclusions (Fig. 4, B and D). Furthermore, SAP mice exhibited severe rough endoplasmic reticulum (rER) damage and reduced number of ribosomes, and significant autophagosome formation in pancreatic acinar cells (Fig. 4, B and D), and damaged lamellar bodies (LBs) with decreased number of LBs in the lung AT II cells (Fig. 4F), when compared with control mice. These provided direct evidence of severe pancreatic and lung injury in the SAP model.

Total and inflammatory cells in BALF

We examined total and inflammatory cells, e.g., macrophages and neutrophils in the BALF from experimental mice. As shown in Figure 5A, Cntl mice contained only alveolar macrophages in BALF, KO mice have higher number of macrophages with foamy alveolar macrophages (Fig. 5D, $P < 0.05$, KO vs. TW and hTG); however, SAP mice included a larger number of neutrophils in BALF of all three types of mice. The quantitative analysis of total cells and inflammatory cells in BALF reveals significant increases in the number of total cells and neutrophils in the SAP WT, KO, and hTG mice compared with Cntl mice. Total cell counts in SAP KO mice were larger than SAP WT and hTG mice. In agreement

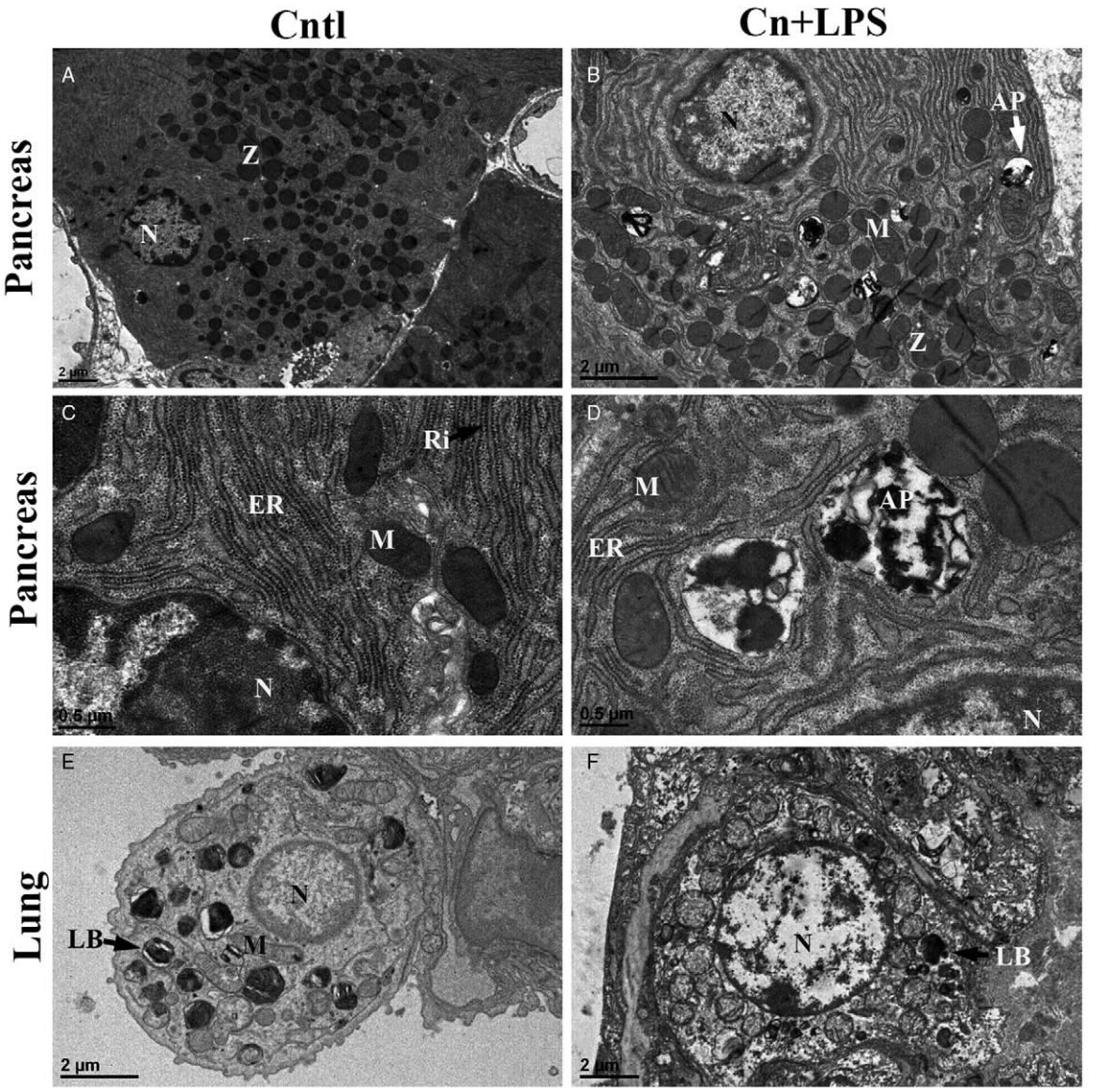

Fig. 4. **Ultrastructural analysis of pancreatic acinar and lung alveolar type II cells by TEM.** Pancreas and lung tissues were fixed and analyzed by transmission electronic microscopy (TEM). Representative ultrastructural properties of pancreatic acinar cells (A–D) and lung alveolar epithelial type II cells (E, F) are shown here. Pancreatic acinar cells exhibited cystic expansion of endoplasmic reticulum, mitochondrial swelling (B), and autophagosome formation (D) in SAP mice but not in control mice (A, C). Severe damaged mitochondria, rough endoplasmic reticulum (rER), and nucleus with reduced number of ribosomes and increased autophagosomes in the pancreatic acinar cells in SAP mice (B, D) but not in control mice. AT II cells in control mice exhibited normal nucleus, mitochondria, and lamellar bodies (E). Severe damaged lamellar bodies (LBs) with decreased number of LBs and damaged nucleus and mitochondria in the AT II cells of SAP mice (F). N, nucleus; M, mitochondria; ER, endoplasmic reticulum; LB, lamellar body; Ly, lysosome; Ri, ribosomes; Z, zymogen granules; AP, autophagy. Scale bars are shown in the photos.

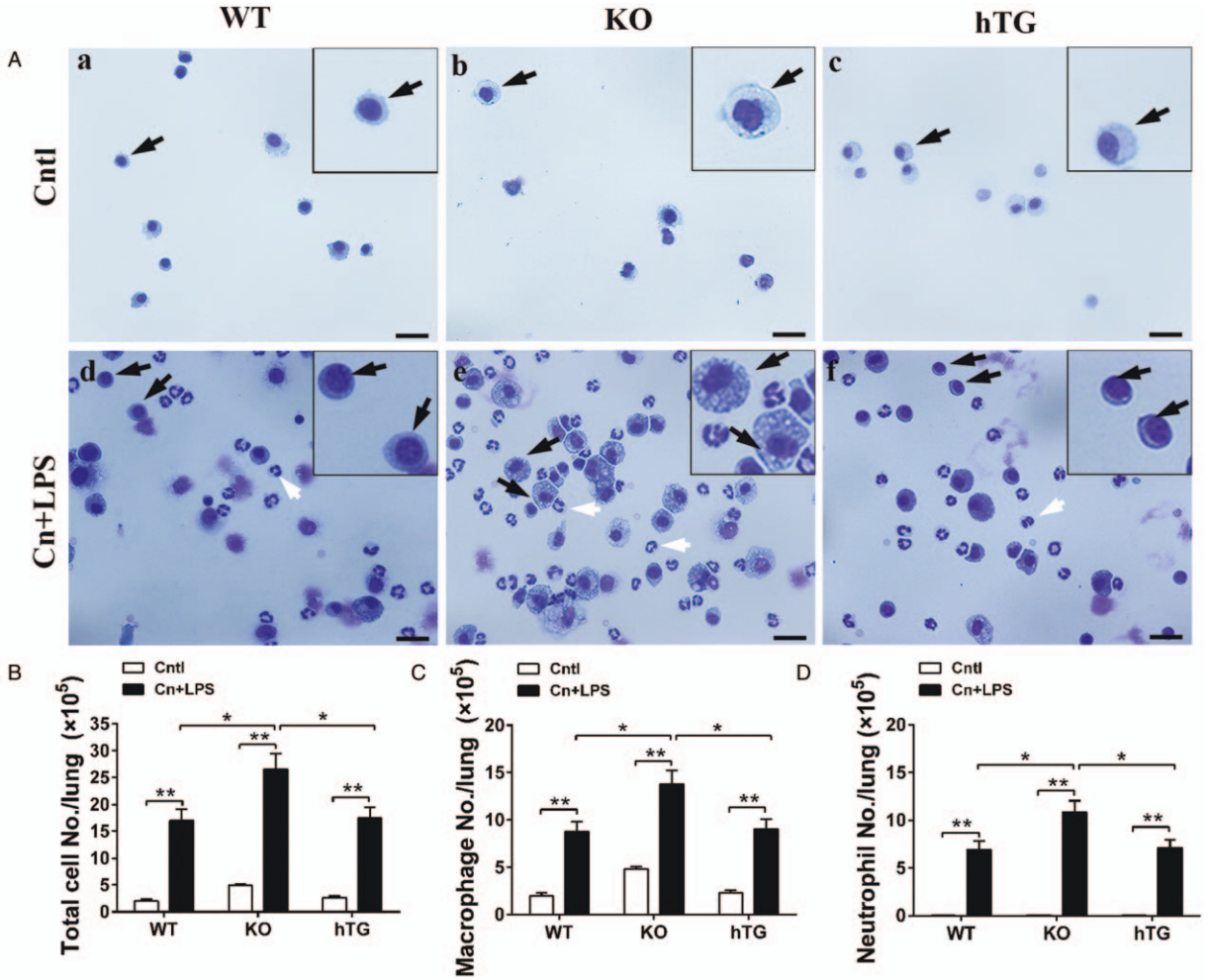

FIG. 5. **Total and inflammatory cells in the BALF in WT, KO, and hTG mice.** Slides containing cells from BALF from control and SAP mice (WT, KO, and hTG) were prepared by cytospin centrifugation and then stained by HEMA-3 staining (A). Macrophages (black arrows) and neutrophils (white arrows) were identified in the slides. Total cell number in the BALF from each mouse were determined with a hemocytometer method. The total cell number (B), macrophages (C) and neutrophils (D) from control and SAP WT, KO, and hTG mice are compared. Graphs are expressed as means ± SEM; n = 4. $^{*}P < 0.05$; $^{**}P < 0.01$. (Original magnification ×400, scale bars = 100 μm).

with the total cell counts, macrophages and neutrophils in SAP KO mice were more than SAP WT and hTG mice (Fig. 5, C and D), suggesting that SP-D plays a critical role in the regulation of inflammation in the lung of SAP model.

SP-D decreased lung neutrophil infiltration and IL-1β expression, and serum cytokines in SAP model

We examined the effects of SP-D on lung neutrophil infiltration and IL-1β expression in SAP WT, KO, and hTG mice. Pulmonary neutrophils were detected using immunofluorescence staining with an anti-MPO (Fig. 6A). The results demonstrated increased neutrophil infiltration in the lung of SAP WT, KO, and hTG mice compared with Cntl mice. The results from quantitative analysis indicated that SAP KO mice have larger number of neutrophils in the lung tissue than SAP WT and hTG (Fig. 6B, KO vs. WT and hTG, $P < 0.01$). We also examined IL-1β expression using immunofluorescence staining with anti-IL-1β antibody (a downstream cytokine of NLRP3 and NF-κB) in this study (Fig. 6C). The results showed that SP-D decreased the IL-1β expression in the lung, e.g., KO mice showed more IL-1β positive cells in the lung than WT and hTG mice (Fig. 6D, $P < 0.01$).

MCP-1, i.e., CCL2 is one of the key chemokines that regulate migration and infiltration of monocytes/macrophages (28). To study SP-D role in the regulation of systematic inflammation, we examined the levels of serum proinflammatory cytokines, e.g., IL-1β and IL-6, and chemokine MCP-1. In agreement with lung inflammation, increased levels of serum IL-1β, IL-6, and MCP-1 were found in SAP KO mice compared with SAP WT and hTG mice (Fig. 7). These indicated that SP-D played a critical role in pulmonary neutrophil infiltration and inflammation in the SAP model.

NLRP3 inflammasome and NF-kB signaling activations are increased in the absence of SP-D

Accumulated evidence has revealed that the NLRP3 inflammasome and NF-κB pathways are essential for the development of ALI. To test the effect of SP-D on pulmonary NLRP3 inflammasome and NF-κB activations after Cn plus LPS-

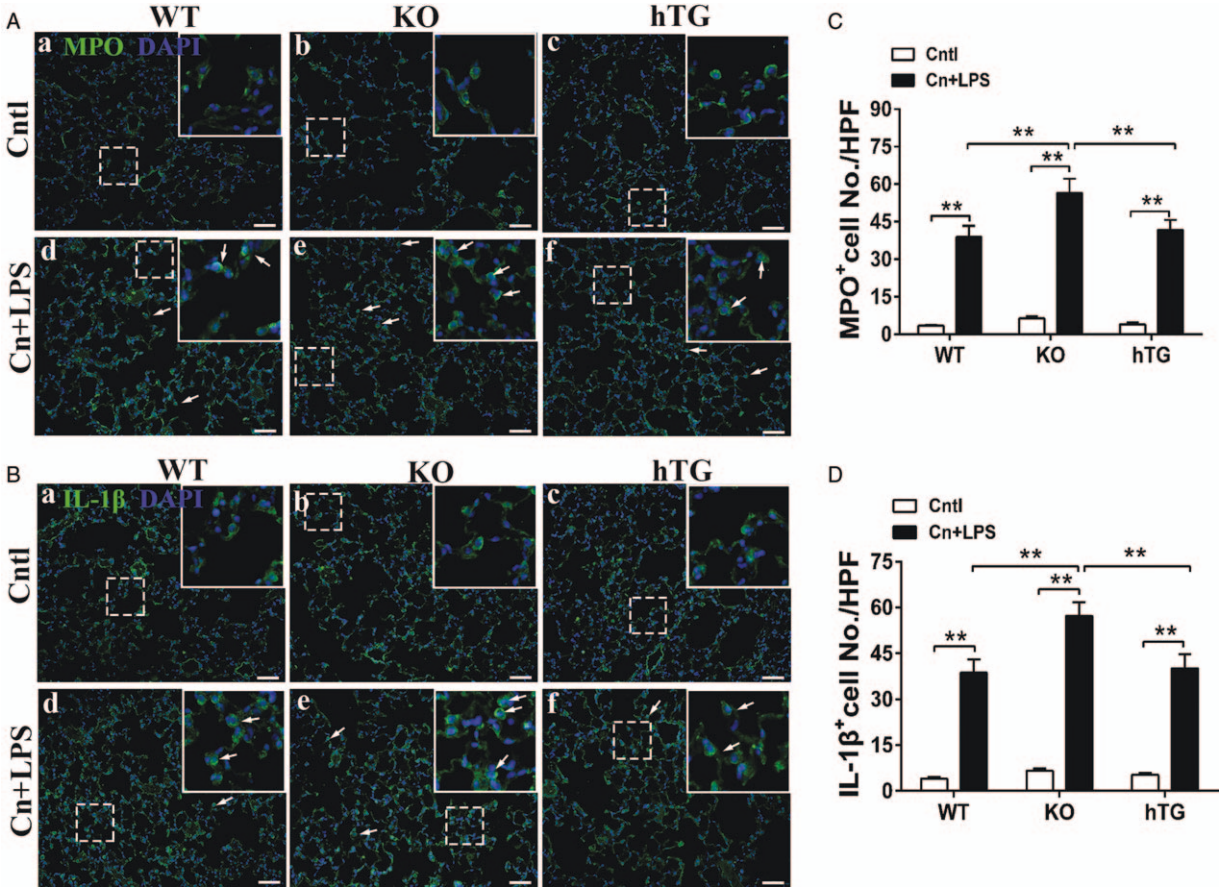

Fig. 6. **Comparison of MPO and IL-1β positive cells in the lung of SAP WT, KO, and hTG mice.** Pulmonary MPO and IL-1β positive cells were detected using immunofluorescence staining in the section of lung from control and SAP WT, KO, and hTG mice. Representative immunofluorescence staining of MPO positive in control and pancreatitis groups of WT, KO, and hTG mice (A). Quantitative analysis of MPO^+ cells of WT, KO, and hTG mice (B). Representative immunofluorescence staining of IL-1β positive in control and pancreatitis groups of WT, KO, and hTG mice (C). Quantitative analysis of $IL\text{-}1\beta^+$ cells of WT, KO, and hTG mice (D). Results are expressed as mean ± SEM; n = 5. $^{**}P < 0.01$. (Original magnification x400, scale bars = 200 μm).

induced pancreatitis, immunofluorescence analyses with an anti-NLRP3 and anti-p-NF-κB p65 (p-p65) antibodies were performed in this study. The results showed that increased NLRP3 inflammasome activation was observed in the cytoplasm of lung AT II cells, macrophages and neutrophils in SAP WT, KO, and hTG mice, but few positive cells in controls (Fig. 8A). We quantified the number of cells with NLRP3 positive, indicating significant increase in the SAP KO mice when compared with SAP WT and hTG mice (Fig. 8B, $P < 0.05$, KO vs. WT and hTG). Similarly, increased number of cells with p-p65 positive were observed in the AT II cells, macrophages and neutrophils in SAP mice but not in controls (Fig. 8C). Quantitative analysis of p-p65 positive cells indicated significant increase in the SAP KO mice compared with SAP WT and hTG mice (Fig. 8D, $P < 0.01$, KO vs. WT and hTG).

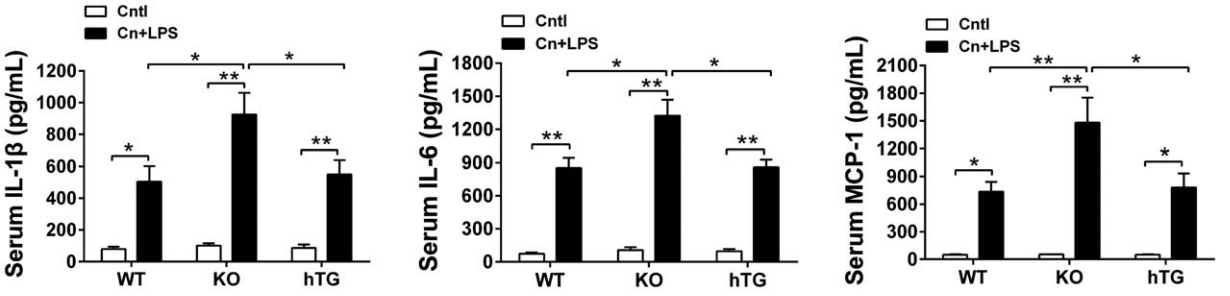

Fig. 7. **Comparison of the levels of serum inflammatory cytokines and chemokine MCP-1 in SAP WT, KO, and hTG mice.** Serum proinflammatory cytokines IL-1β and IL-6 levels were measured in SAP WT, KO, and hTG mice, as well as controls by ELISA. The levels of serum IL-1β (A), IL-6 (B), and MCP-1 (C) were elevated in the SAP mice 24 h after treatment compared with controls. SAP KO mice showed increased expression compared SAP WT and hTG mice. Graphs are expressed as Mean ± SEM; n = 5. $^{*}P < 0.05$; $^{**}P < 0.01$.

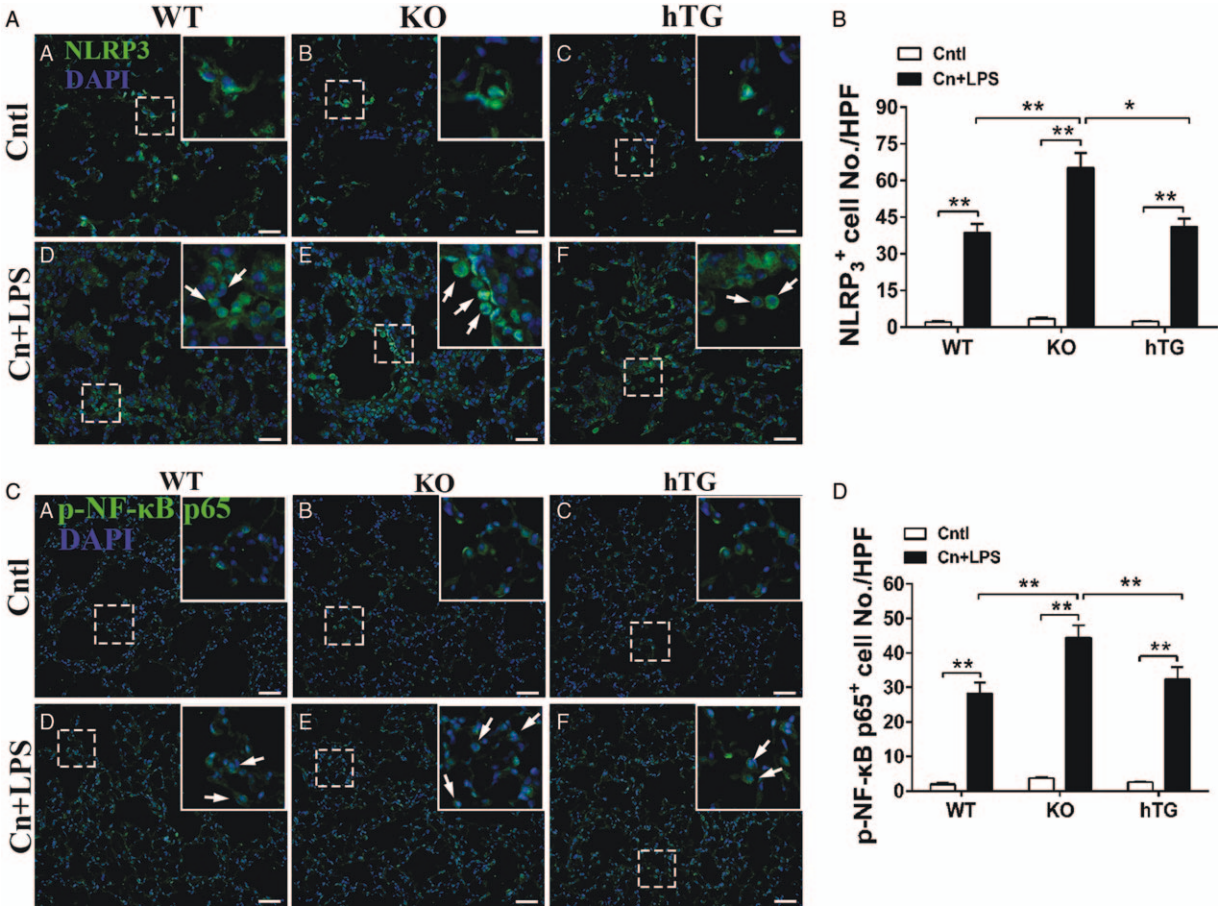

FIG. 8. **Effects of SP-D on NOD-like receptor protein 3 (NLRP3) inflammasome formation and NF-κB expression in the lung of SAP mice.** NLRP3 inflammasomes were detected by immunofluorescence staining with NLRP3 antibody in the lung section of SAP WT, KO, and hTG mice, as well as controls (A). The cell number of $NLRP_3^+$ were quantified and compared in the lung sections of SAP WT, KO, and hTG mice, as well as controls (B). NF-κB nucleus translocation was assessed using fluorescence microscopy to determine the nuclear localization of p-p65 following acute pancreatitis (C) and quantitative analysis (D). Results are expressed as mean ± SEM; n = 5. $^*P < 0.05$; $^{**}P < 0.01$. (Original magnification ×400, scale bars = 200 μm).

To further study the correlation between NLRP3 inflammasome and NF-κB signaling activations and SP-D expression in SAP mice, we examined the NLRP3 inflammasome and NF-κB signaling activation in the lung tissue of KO, WT, and hTG mice by Western blotting analysis. The results showed that the association of the complex of NLRP3, ASC, and Caspase-1 in the lung substantially increased after the administration of Cn and LPS (Fig. 9A). Increased the activation of the NLRP3 inflammasome was observed in the SAP KO mice compared with SAP WT and hTG mice, suggesting that SP-D suppressed the activation of the NLRP3 inflammasome in the SAP model (Fig. 9B). Phosphorylation of IκB-α is required for the initiation of NF-κB signaling activation. Hence, the levels of phosphorylated IκB-α (p-IκB-α) and p-p65 in the lung were examined. As shown in Figure 9C, there was a significant increase in the levels of p-IκB-α and p-p65 in SAP mice 24 h after Cn plus LPS treatment compared with control mice. Importantly, the levels of p-IκB-α and p-p65 in the lung from SAP KO mice were higher than SAP WT mice and hTG mice (Fig. 9D). These results indicated that SP-D is involved in the regulation of NLRP3 inflammasome and NF-κB signaling activation and play a critical role in the pathogenesis of SAP.

DISCUSSION

AP accompanied by a subsequent infectious attack often leads to systemic inflammation and multiple organ failure. SAP causes a high mortality rate (15%–20%), hence AP is an intricate problem in clinical management (2). Among the systemic complications, ALI is considered as the most frequent and severe complication and is indeed the predominant cause of death in the patients with SAP (2). The molecular mechanisms of AP-induced ALI are rather complicated and remain poorly understood; therapeutic remedies targeting the inflammatory modulators seem to be the most appropriate approaches for treating AP and AP-induced ALI (8). Humanized transgenic mice which express lung-specific human SP-D but without mouse SP-D background allow us to study SP-D effect in the lung in SAP model. Here, we for the first time present evidence that SP-D is involved in the regulation of inflammation through

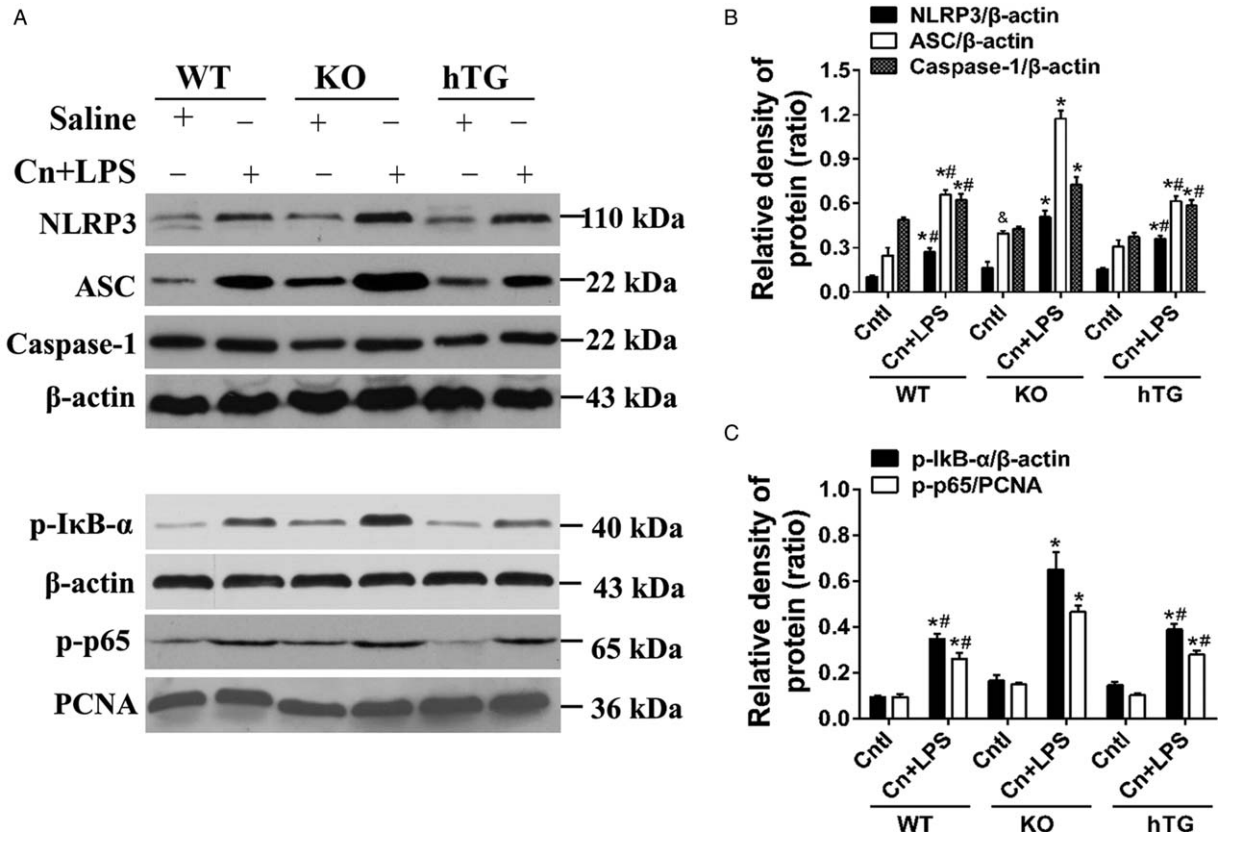

Fig. 9. **Role of SP-D on components of NLRP3 inflammasome complex and NF-κB activation in the lung of SAP mice.** Lung tissues from experimental and control groups were prepared from SAP WT, KO, and hTG mice and controls at 24 h after treatment. Representative western blots of NLRP3, ASC, cleaved Caspase-1 protein (three important components of the inflammasome formation) expressions are shown (A). (B) Quantitative analysis of NLRP3, ASC, and active Caspase-1. (C) The protein levels of p-IκB-α, and p-p65. (D) Quantitative analysis of p-IκBα and p-p65. Results are expressed as mean ± SEM; n = 3. $^{*}P < 0.05$ SAP group vs. respective Cntl group; $^{\#}P < 0.05$ SAP WT or SAP hTG vs. SAP KO group; $^{\&}P < 0.05$ Cntl KO vs. Cntl WT group.

modulating NF-kB signaling and NLRP3 inflammasome activations in SAP-induced ALI.

In the present study we have tested a ''two-hit'' SAP model with WT, SP-D KO, and hTG mice, in which SAP was induced by 6-time Cn injections and a single-dose LPS secondary insult. We found that Cn plus LPS-induced SAP mice exhibited remarkable acute pancreatic and lung injury by assessments of various histological, serum biochemical, cellular, and molecular changes. The characteristics of pancreatic and lung injury in the SAP model are similar to those in the patients with SAP, including pancreatic edema, inflammation, and necrosis of the acinar cells, as well as acute lung inflammation and injury. Of interest, mice lacking SP-D expression showed more severe pancreatic and lung injury when compared with WT mice. Although human SP-D protein was expressed in the lung of hTG mice, the degree of injury in both pancreas and lung was lower than SP-D KO mice, suggesting that SP-D plays an important role in the pathogenesis of SAP. Furthermore, our ultrastructural analysis by TEM demonstrated severe mitochondrial and rough endoplasmic reticulum damage, and significantly reduced number of ribosomes, and increased autophagosome formation in the pancreatic acinar cells, and reduced normal LBs in the AT II cells in SAP mice. The ultrastructural changes of acinar cells and AT II cells provided direct evidence of cellular damages in the pancreas and lung of the SAP.

SP-D, a multimeric collectin, is involved in innate immunity and regulation of inflammation in the lung, as well as extrapulmonary tissues such as pancreas, bile duct, gallbladder, and kidney (19). Although SP-D has been intensively studied in the surfactant biology, host defense, and homeostasis in the lung, recent studies from us and others demonstrated its critical roles in the extrapulmonary tissues, including attenuating sepsis-induced kidney and intestine injuries (23), as well as regulating gut commensal bacterial homeostasis in an experimental IBD model (29). These indicate that SP-D may play broad roles in the inflammatory regulation of different diseases, thus being as an appropriate therapeutic target.

In this study we have observed severe SAP-induced ALI. Importantly, SAP KO mice showed more severe lung injury, and more inflammatory macrophages and neutrophils in BALF than SAP WT and hTG mice. Neutrophil activation occurs as a result of complement activation, cytokine production, adhesion molecule expression, and alveolar macrophage activation (30). Activated neutrophils in the lung release proteolytic enzymes and produce reactive oxygen species (ROS) that contribute to the development of ALI (31). As reported, the severity of ALI is correlated with two interdependent processes: the recruitment of inflammatory cells and the upregulation of proinflammatory cytokines (10). Our data demonstrate that SP-D inhibited lung inflammation in SAP, including the infiltration of inflammatory

cells (neutrophils, macrophages) and the overproduction of important proinflammatory cytokines (IL-6, IL-1β and MCP-1). In addition to its antioxidative property (32), SP-D mediated alleviation of lung injury was also derived from the reduction of these inflammatory components. MPO activity has been recognized as an indicator of determining quantitatively the extent of neutrophils infiltration. IL-1β is required for full distant organ injury in experimental SAP model (12). We observed that Cn plus LPS stimulation caused significant activation and infiltration of neutrophils and inflammatory cytokine, which could be reversed by transgenic SP-D expression in hTG mice. Although higher level of hSP-D in the lung of hTG mice was detected by western blotting analysis when compared with WT mice, no difference of response was found between hTG and WT mice in the SAP model. It may be caused by differential affinity to human SP-D protein with the antibody or due to functional difference of hSP-D and mouse SP-D. These demonstrate that SP-D played an important regulatory role in pulmonary neutrophil infiltration and inflammation response in the SAP.

Inflammation is the first response of the immune system to infection or tissue injury to protect the body from those insults (33). Among the various inflammatory responses in the lung, NLRP3 inflammasome and NF-κB signaling activations are important (10). Many proteins of the NOD-like receptor (NLR) family have been identified as central players in innate immunity, NLRP3 inflammasome is a protein complex involved in IL-1β and IL-18 processing that senses pathogen- and danger-associated molecular patterns (PAMPs and DAMPs) (11). NF-κB is normally composed of the p50/p65 heterodimers that is sequestered in the cytosol in the quiescent state by association with the IκB inhibitors. Upon stimulation, IκB is phosphorylated and then dissociates from NF-κB complex, allowing the free phosphorylated NF-κB to translocate into the nucleus and triggering expression of many types of cytokines and inflammation-related genes (34). In this study we observed increased activation of NLRP3 and p-NF-κB p65 in lung in SAP mice. SP-D in WT and hTG mice is able to significantly reduce the activations of lung NLRP3 inflammasome and p-NF-κB p65. Furthermore, molecular analysis demonstrated that increased levels of components of NLRP3 Complex (NLRP3, ASC, and Caspase-1) as well as the p-IκB and p-p65 in the lung of SAP KO mice compared with SAP WT and hTG mice, suggesting the role of SP-D in suppressing NLRP3 inflammasome and NF-κB signaling activations.

Inflammation can be triggered by a battery of receptors recognizing molecular structures specific to PAMPs from microorganisms or signals from DAMPs. These receptors are highly diverse in their specificities, subcellular localizations, and downstream signaling pathways, and constitute a network able to trigger an appropriate response to a large variety of insults (11, 33, 35). NLRP3 can respond to not only PAMPs such as gram-negative bacteria and toxins but also a wide range of endogenous and exogenous DAMPs such as uric acid, ATP, and ROS (35). These DAMPs originate from multiple sources, including injured and dying cells, the extracellular matrix, or exist as immunomodulatory proteins within the airspace and interstitium (33). Immunomodulatory proteins, such as β-defensins and SP-A and SP-D, are involved in a variety of biological processes, including host defense and lung physiology (36). DAMPs can function as either toll-like receptor (TLR) agonists or antagonists, and can modulate both TLR and NLR signaling cascades. Previous studies demonstrated that SP-D could interact with TLR2 and TLR4, and inhibit TLRs-mediated cytokine production and recruitment of PMNs (33). The lack of functional TLR4 lead to a blunted NF-κB response, reduced proinflammatory mediator production, and ameliorated lung inflammation in mice and alveolar macrophages (37). Moreover, NF-κB signaling is an essential initial step for priming of NLRP3 activation, and ROS generated from NF-κB-mediated inflammation also serves as a danger signal that activates NLRP3 (38). NLRP3 forms an inflammasome complex and responds to a wide range of infections and stress stimuli (35). Once NLRP3 becomes activated, there ensues the recruitment of ASC, activation of caspase-1, and processing of pro-IL-1β into mature forms ensues (11). SP-D is involved in the regulation of NF-κB signaling pathway in sepsis-induced acute pancreatic and kidney injury (22, 23). Chemokines are secreted in response to signals such as proinfammatory cytokines where they play an important role in selectively recruiting monocytes, neutrophils, and lymphocytes (28). MCP-1, as a well-known chemokine and a direct target of NF-kB, has been demonstrated to be induced and involved in various diseases including AP (13, 28). The findings in this study indicate that SP-D played inhibitory effects on both the NLRP3 and NF-κB signaling pathways, and reduced the expression of cytokines IL-1β and IL-6, and chemokine MCP-1 in the SAP model. Although NF-kB signaling is vital to NLRP3 activation, the process of NLRP3 inflammasome formation and activation is extremely complicated in response to various insults. It is unclear how SP-D regulates activation of NLRP3 inflammasome by either direct interaction with the NLRPL3 inflammasome or indirect effects via other priming signals, which remains to be further studied in the future.

In summary, we demonstrated that SP-D dampened SAP-induced ALI as well as pancreatic injury in an experimental SAP model. The mechanisms underlying this protective effect might include the inhibition of NLRP3 inflammasome and NF-κB signaling activations. These findings support the notion that SP-D may be a potential target for treating SAP and SAP-induced ALI.

REFERENCES

1. Buter A, Imrie C, Carter C, Evans S, McKay C: Dynamic nature of early organ dysfunction determines outcome in acute pancreatitis. *Br J Surg* 89(3):298–302, 2002.
2. De Campos T, Deree J, Coimbra R: From acute pancreatitis to end-organ injury: mechanisms of acute lung injury. *Surg Infect (Larchmt)* 8(1):107–120, 2007.
3. Matthay MA, Ware LB, Zimmerman GA: The acute respiratory distress syndrome. *J Clin Investigation* 122(8):2731–2740, 2012.
4. Gukovskaya AS, Gukovsky I, Algul H, Habtezion A: Autophagy, inflammation, and immune dysfunction in the pathogenesis of pancreatitis. *Gastroenterology* 153(5):1212–1226, 2017.
5. Hoque R, Farooq A, Ghani A, Gorelick F, Mehal WZ: Lactate reduces liver and pancreatic injury in Toll-like receptor–and inflammasome-mediated inflammation via GPR81-mediated suppression of innate immunity. *Gastroenterology* 146(7):1763–1774, 2014.
6. Hoque R, Sohail M, Malik A, Sarwar S, Luo Y, Shah A, Barrat F, Flavell R, Gorelick F, Husain S: TLR9 and the NLRP3 inflammasome link acinar cell

death with inflammation in acute pancreatitis. *Gastroenterology* 141(1):358–369, 2011.
7. Tian X, Sun H, Casbon AJ, Lim E, Francis KP, Hellman J, Prakash A: NLRP3 inflammasome mediates dormant neutrophil recruitment following sterile lung injury and protects against subsequent bacterial pneumonia in mice. *Front Immunol* 8:1337, 2017.
8. Lin ZS, Ku CF, Guan YF, Xiao HT, Shi XK, Wang HQ, Bian ZX, Tsang SW, Zhang HJ: Dihydro-resveratrol ameliorates lung injury in rats with cerulein-induced acute pancreatitis. *Phytother Res* 30(4):663–670, 2016.
9. Sarma JV, Ward PA: Oxidants and redox signaling in acute lung injury. *Compr Physiol* 1(3):1365–1381, 2011.
10. Liu Q, Lv H, Wen Z, Ci X, Peng L: Isoliquiritigenin activates nuclear factor erythroid-2 related factor 2 to suppress the NOD-like receptor protein 3 inflammasome and inhibits the NF-kappaB pathway in macrophages and in acute lung injury. *Front Immunol* 8:1518, 2017.
11. Kim YK, Shin J-S, Nahm MH: NOD-like receptors in infection, immunity, and diseases. *Yonsei Med J* 57(1):5–14, 2016.
12. Granger J, Remick D: Acute pancreatitis: models, markers, and mediators. *Shock* 24(Suppl. 1):45–51, 2005.
13. Zhou GX, Zhu XJ, Ding XL, Zhang H, Chen JP, Qiang H, Zhang HF, Wei Q: Protective effects of MCP-1 inhibitor on a rat model of severe acute pancreatitis. *Hepatobiliary Pancreat Dis Int* 9(2):201–207, 2010.
14. Jiang L, Zhang L, Kang K, Fei D, Gong R, Cao Y, Pan S, Zhao M, Zhao M: Resveratrol ameliorates LPS-induced acute lung injury via NLRP3 inflammasome modulation. *Biomed Pharmacother* 84:130–138, 2016.
15. Nguyen HA, Rajaram MV, Meyer DA, Schlesinger LS: Pulmonary surfactant protein A and surfactant lipids upregulate IRAK-M, a negative regulator of TLR-mediated inflammation in human macrophages. *Am J Physiol Lung Cell Mol Physiol* 303(7):L608–L616, 2012.
16. Wright JR: Immunoregulatory functions of surfactant proteins. *Nat Rev Immunol* 5(1):58, 2005.
17. Madsen J, Kliem A, Tornoe I, Skjodt K, Koch C, Holmskov U: Localization of lung surfactant protein D on mucosal surfaces in human tissues. *J Immunol* 164(11):5866–5870, 2000.
18. Kishore U, Greenhough TJ, Waters P, Shrive AK, Ghai R, Kamran MF, Bernal AL, Reid KB, Madan T, Chakraborty T: Surfactant proteins SP-A and SP-D: structure, function and receptors. *Mol Immunol* 43(9):1293–1315, 2006.
19. Sorensen GL: Surfactant protein D in respiratory and non-respiratory diseases. *Front Med (Lausanne)* 5:1–37, 2018.
20. Grailer JJ, Canning BA, Kalbitz M, Haggadone MD, Dhond RM, Andjelkovic AV, Zetoune FS, Ward PA: Critical role for the NLRP3 inflammasome during acute lung injury. *J Immunol* 192(12):5974–5983, 2014.
21. Zhu T, Wang D-x, Zhang W, Liao X-q, Guan X, Bo H, Sun J-y, Huang N-w, He J, Zhang Y-k: Andrographolide protects against LPS-induced acute lung injury by inactivation of NF-κB. *PLoS One* 8(2):e56407, 2013.
22. Liu Z, Shi Q, Liu J, Abdel-Razek O, Xu Y, Cooney RN, Wang G: Innate immune molecule surfactant protein D attenuates sepsis-induced acute pancreatic injury through modulating apoptosis and NF-kappaB-mediated inflammation. *Sci Rep* 5:17798, 2015.
23. Liu J, Abdel-Razek O, Liu Z, Hu F, Zhou Q, Cooney RN, Wang G: Role of surfactant proteins A and D in sepsis-induced acute kidney injury. *Shock)* 43(1):31, 2015.
24. Zhang X, Shi Q, Wang C, Wang G: Differential susceptibility of mouse strains on pancreatic injury and regeneration in cerulein-induced pancreatitis. *Int J Clin Exp Pathol* 10(9):9934–9944, 2017.
25. Kubisch C, Dimagno MJ, Tietz AB, Welsh MJ, Ernst SA, Brandt-Nedelev B, Diebold J, Wagner AC, Goke B, Williams JA, et al.: Overexpression of heat shock protein Hsp27 protects against cerulein-induced pancreatitis. *Gastroenterology* 127(1):275–286, 2004.
26. Matute-Bello G, Downey G, Moore BB, Groshong SD, Matthay MA, Slutsky AS, Kuebler WM, Acute Lung Injury in Animals Study G. An official American Thoracic Society workshop report: features and measurements of experimental acute lung injury in animals. *Am J Respir Cell Mol Biol* 44(5):725–738, 2011.
27. Wang G, Guo X, Diangelo S, Thomas NJ, Floros J: Humanized SFTPA1 and SFTPA2 transgenic mice reveal functional divergence of SP-A1 and SP-A2: formation of tubular myelin in vivo requires both gene products. *J Biol Chem* 285(16):11998–12010, 2010.
28. Deshmane SL, Kremlev S, Amini S, Sawaya BE: Monocyte chemoattractant protein-1 (MCP-1): an overview. *J Interferon Cytokine Res* 29(6):313–326, 2009.
29. Sarashina-Kida H, Negishi H, Nishio J, Suda W, Nakajima Y, Yasui-Kato M, Iwaisako K, Kang S, Endo N, Yanai H, et al.: Gallbladder-derived surfactant protein D regulates gut commensal bacteria for maintaining intestinal homeostasis. *Proc Natl Acad Sci USA* 114(38):10178–10183, 2017.
30. Closa D, Sabater L, Fernandez-Cruz L, Prats N, Gelpi E, Rosello-Catafau J: Activation of alveolar macrophages in lung injury associated with experimental acute pancreatitis is mediated by the liver. *Ann Surg* 229(2):230–236, 1999.
31. Shields CJ, Winter DC, Redmond HP: Lung injury in acute pancreatitis: mechanisms, prevention, and therapy. *Curr Opin Crit Care* 8(2):158–163, 2002.
32. Yoshida M, Korfhagen TR, Whitsett JA: Surfactant protein D regulates NF-(B and matrix metalloproteinase production in alveolar macrophages via oxidant-sensitive pathways. *J Immunol* 166(12):7514–7519, 2001.
33. Tolle LB, Standiford TJ: Danger-associated molecular patterns (DAMPs) in acute lung injury. *J Pathol* 229(2):145–156, 2013.
34. Chow C-W, Herrera Abreu MT, Suzuki T, Downey GP: Oxidative stress and acute lung injury. *Am J Respir Cell Mol Biol* 29(4):427–431, 2003.
35. Place DE, Kanneganti TD: Recent advances in inflammasome biology. *Curr Opin Immunol* 50:32–38, 2018.
36. Sloane JA, Blitz D, Margolin Z, Vartanian T: A clear and present danger: endogenous ligands of Toll-like receptors. *Neuromolecular Med* 12(2):149–163, 2010.
37. Joh E-H, Gu W, Kim D-H: Echinocystic acid ameliorates lung inflammation in mice and alveolar macrophages by inhibiting the binding of LPS to TLR4 in NF-(B and MAPK pathways. *Biochem Pharmacol* 84(3):331–340, 2012.
38. Bauernfeind F, Horvath G, Stutz A, Alnemri ES, MacDonald K, Speert D, Fernandes-Alnemri T, Wu J, Monks BG, Fitzgerald KA, et al.: NF-kB activating pattern recognition and cytokine receptors license NLRP3 inflammasome activation by regulating NLRP3 expression. *J Immunol* 183(2):787–791, 2009.